POLITECNICO DI TORINO
Repository ISTITUZIONALE

Hybrid Multi-Criteria Decision Making for Additive or Conventional Process Selection in the Preliminary Design Phase

Original
Hybrid Multi-Criteria Decision Making for Additive or Conventional Process Selection in the Preliminary Design Phase / Salmi, A., Vecchi, G., Atzeni, E., Iuliano, L.. - In: DESIGNS. - ISSN 2411-9660. - ELETTRONICO. - 8:6(2024). [10.3390/designs8060110]

Availability:
This version is available at: 11583/2993204 since: 2024-10-29T14:47:50Z

Publisher:
MDPI

Published
DOI:10.3390/designs8060110

Terms of use:

This article is made available under terms and conditions as specified in the corresponding bibliographic description in the repository

Publisher copyright

(Article begins on next page)

12 October 2026

MDPI

Article

Hybrid Multi-Criteria Decision Making for Additive or Conventional Process Selection in the Preliminary Design Phase

Alessandro Salmi, Giuseppe Vecchi *, Eleonora Atzeni and Luca Iuliano

Department of Management and Production Engineering (DIGEP), Politecnico di Torino, Corso Duca degli Abruzzi 24, 10129 Torino, Italy; alessandro.salmi@polito.it (A.S.); eleonora.atzeni@polito.it (E.A.); luca.iuliano@polito.it (L.I.)

* Correspondence: giuseppe_vecchi@polito.it; Tel.:+39-011-090-7263

Abstract: Additive manufacturing (AM) has become a key topic in the manufacturing industry, challenging conventional techniques. However, AM has its limitations, and understanding its convenience despite established processes remains sometimes difficult, especially in preliminary design phases. This investigation provides a hybrid multi-criteria decision-making method (MCDM) for comparing AM and conventional processes. The MCDM method consists of the Best-Worst-Method (BWM) for the definition of criteria weights and the Proximity Index Value (PIV) method for the generation of the final ranking. The BWM reduces the number of pairwise comparisons required for the definition of criteria weights, whereas the PIV method minimises the probability of rank reversal, thereby enhancing the robustness of the results. The methodology was validated through a case study, an aerospace bracket. The candidate processes for the bracket production were CNC machining, high-pressure die casting, and PBF-LB/M. The production of the bracket by AM was found to be the optimal choice for small to medium production batches. Additionally, the study emphasised the significance of material selection, process design guidelines, and production batch in the context of informed process selection, thereby enabling technical professionals without a strong AM background in pursuing conscious decisions.

Keywords: Additive Manufacturing; DfAM; PBF-LB; CNC machining; HPDC; Hybrid MCDM; BWM; PIV;

Citation: Salmi, A.; Vecchi, G.; Atzeni, E.; Iuliano, L. Hybrid Multi-Criteria Decision Making for Additive or Conventional Process Selection in the Preliminary Design Phase. *Designs* **2024**, *1*, 0. https://doi.org/

Received:
Revised:
Accepted:
Published:

Copyright: © 2024 by the authors. Submitted to *Designs* for possible open access publication under the terms and conditions of the Creative Commons Attri- bution (CC BY) license (https://creativecommons.org/licenses/by/4.0/).

1. Introduction

The activity of producing a component is a crucial step in the manufacturing workflow, beginning with the conception of an idea and culminating with its realisation [1]. As concerns manufacturing, it has traditionally been divided into *mass conserving* and *mass reducing* processes, depending on whether they retain the initial provided mass or not [1]. Nowadays, these categories should be expanded to include *mass increasing* processes, typical of the Additive Manufacturing (AM) industry. AM fabricates parts by adding material layer-by-layer until the final desired shape is met [2]. AM originated in the late 1980s as Rapid Prototyping (RP), primarily concerning the fast production of polymeric prototypes. Over the decades, it has evolved into an actual manufacturing process able to produce market-ready metallic parts [3]. The AM family of manufacturing processes can overcome many constraints of conventional manufacturing (CM) processes that have long limited designers' concepts [4]. The most critical of these limits are the need for specific tools for each manufacturing step, the cost of a part being strictly dependent on its geometrical complexity [5], and the need for many sequential processes to achieve the net shape of a component [6]. However, designers should be aware that new possibilities also bring new constraints and limitations. AM systems are strongly limited by the scarcity of dedicated materials, modest working volumes, and prolonged fabrication times [7]. Additionally, AM processes cannot provide the same quality ensured by machining operations in terms of dimensional tolerances, geometrical tolerances, and surface roughness [8]. Although

AM processes have been previously proposed as holding several competitive advantages over conventional ones, it is not straightforward to decide if a component should or should not be realised by AM, and which AM process to consider [9].

Each manufacturing process requires tailored design considerations. Therefore, it is straightforward that the manufacturing process should be uniquely defined during the design phase to be fed with an appropriately shaped component. Understanding which is the most suitable manufacturing process for the production of a component is still a demanding activity, requiring high level knowledge by the operator in charge. A powerful tool supporting the process selection is represented by Multiple-Criteria Decision Making (MCDM) methods [10], enabling the comparison of different conflicting criteria coming from different fields [11]. Currently, several methods have been already profitably used in MCDM field, such as the Analytic Hierarchy Process (AHP), Technique for Order of Preference by Similarity to Ideal Solution (TOPSIS) and VIKOR methods [12], whereas new MCDM methods such as the Best Worst Method (BWM) and the Proximity Index Value (PIV) are rising to the attention [13,14].

MCDM methods have been successfully implemented in the AM industry for various objectives, including material selection [15], part design selection [16,17] and part orientation [18]. Moreover, in the AM field, MCDM methods have been extensively utilised for selecting the most suitable AM process. Mançanares et al. [19] proposed a two-step procedure to identify the most suitable AM process based on the requirements of the part. The manufacturability of the component was evaluated based on its size and material, followed by an AHP process selection step which provided the final ranking of AM processes under investigation. Similarly, Liu et al. [20] assessed the manufacturability of the selected component using AM processes, only considering the functional specifications of the part. Subsequently, the remaining AM processes were ranked from the most suitable to the least using the AHP method. Zaman et al. [21] applied the AHP method to define the best solution for producing an aerospace component, considering AM materials, AM processes and AM machine systems. Ghaleb et al. [22] conducted a comparative analysis on the behaviour of AHP, TOPSIS and VICKOR methods to assess the best manufacturing process for the production of a hydraulic pump casing. The study directly compared casting and AM processes, representing the first study in which these two manufacturing paradigms were directly compared.

Furthermore, the proposal of hybrid MCDM methods has significantly increased the reliability of the results obtained. Different MCDM methods can successfully cover various phases of the process selection framework, leveraging their strengths and minimising their weaknesses at the same time. Wang et al. [23] developed a hybrid process selection method to compare different polymeric AM processes. The AHP method was used to weight the considered criteria, and the TOPSIS method was used to compile the final ranking. Wang et al. [24] used a nonlinear fuzzy geometric mean (FGM) approach followed by a fuzzy VIKOR to evaluate the best AM system for the production of an aircraft component, choosing between fused deposition modelling (FDM), PBF-LB and MultiJet Fusion. Grachev et al. [25] assembled a hybrid AHP-TOPSIS method for material selection in AM dental applications. Finally, Raigar et al. [26] employed a hybrid BWM-PIV method to identify the most appropriate AM machine for a given component. The authors compared various polymeric AM processes, such as vat photopolymerisation, material extrusion and material jetting, with metal AM processes, specifically powder bed fusion. The methodology proposed was evaluated on the case study of a conceptual model of spur gear.

Although a clear interest of AM shareholders is demonstrated by the reported studies, no hybrid MCDM methods have been applied to compare AM processes to conventional ones, limiting the investigation to the only AM environment. Most of published investigations have yielded helpful results by means of largely established MCDM methods, AHP, TOPSIS and VIKOR above all. Most recent MCDM, such as the BWM and the PIV method, have been underutilised and never applied to compare AM processes to conventional ones. BWM is claimed to reduce the number of pairwise comparisons between considered

elements, increasing the reliability of the results. PIV might be of great interest in the field of process selection as it claims to minimise the vulnerability of the proposed ranking to the rank reversal phenomenon.

This paper confidently answers a common question every company faces when first considering AM, "Can this component be produced by AM, and is it advantageous to do so?". The authors suggest that a hybrid MCMD method could be used to compare AM with CM processes, expanding its application to a broader range of technologies. Section 2 presents the adopted methodology. The chosen hybrid MCDM method consists of a first linearised BWM method to define attribute weights and PIV method to rank the processes. The BWM guarantees the minimal number of pairwise comparisons during the definition of criteria weights, thereby simplifying the procedure. Furthermore, the PIV method is designed to mitigate the rank reversal problem, thereby ensuring a more robust outcome at the conclusion of the procedure. The resilience of the PIV method to rank reversal is of paramount importance in the proposed methodology, as it accounts for the potential introduction or removal of manufacturing processes during the evaluation, which could occur in a real industrial setting. Finally, an inspiring topology optimisation (TO) phase is also proposed for improving the design of the component, able to improve its suitability in the AM scenario. Section 3 presents a case study coming from the aerospace sector to demonstrate the applicability of the proposed methodology in a real scenario. Finally, Section 4 draws the conclusions of the study, emphasising the most relevant findings.

2. Materials and Methods

The proposed framework is intended to empower industrial figures, without a strong AM background, in evaluating the suitability and convenience of AM processes for the production of a given part out of additive and conventional manufacturing processes. The proposed hybrid MCDM method can easily identify the issues associated with the component at an early stage of the design, prior to its finalisation. This allows for the incorporation of modifications that could enhance its manufacturability. Therefore, allowing engineers and designers to be completely aware of process requirements even at early-design stages.

An overview of the whole methodology is presented in Figure 1. At first, candidate processes are identified based on the functional specifications of the part concept. Both conventional manufacturing processes and AM processes are considered. Subsequently, in the process exploration phase, a first screening is performed to discard unsuitable processes, then the most appropriate process is identified in the process selection phase, through the application of a MCDM method. As results, the manufacturability by AM and its convenience is established, or the AM process is rejected. Details of each phase of the methodology are presented in the following subsections.

2.1. Process Exploration Phase

Once the process candidates have been identified, the initial task is to refine the concept design of the part by applying the process guidelines in order to improve its manufacturability. This is followed by verification of the consistency of the design with the functional specifications. At this stage, the use of software packages may be necessary to perform the numerical simulations required to assess if functional specifications are met. If the compliance with part functional specifications is verified, this phase leads to product/process requirements. Conversely, the process is rejected. These tasks are carried out in parallel for each candidate process. For instance, in the case of an AM process, basic considerations in the design refinement are:

- A commercially available material can be used;
- Overall dimensions of the part fit the building volume (to avoid assembly operations);
- The minimum wall thickness can be achieved;
- The process tolerances meet the required tolerances, or tolerances can be achieved with post-processing operations;

It is possible that some modifications may be required at this stage. Minor details may be altered or a non-processable material may be replaced with a similar one, thereby enhancing the manufacturability of the part. The refined part concept is now capable of being produced by AM. However, in order for the part to be considered for AM, it must also meet the functional specifications in order to properly undergo the requisite working loads during its intended operational lifetime.

2.2. Process Selection Phase

Once the manufacturability of a component has been established for a given set of processes that have successfully completed the exploration phase, the most suitable manufacturing process must be identified. A hybrid MCDM method is employed during the process selection phase. This involves selecting criteria and then assessing the convenience of each manufacturing process based on these criteria. Specifically, when defining criteria, geometry metrics, sustainability, production time and costs are considered. The necessity of exploiting different software packages arises also during the process selection phase. For instance, the definition of the waste material and of the energetic demand, which contribute to the aforementioned sustainability criterion, may require the utilisation of specific software packages with the objective of achieving higher estimate accuracy.

The complexity of the part plays a major role in the process selection framework, especially when dealing with AM processes. Geometrical complexity is often regarded as "for free" in AM applications [27], meaning that the same machine system can be used to manufacture parts of varying geometrical complexity without, or with minimal, additional costs. In this paper, part complexity is computed based on three main parameters:

- *volumetric index*, which is a measure of the amount of the volume occupied by the part within a regular bounding box in which it is contained:

$$I_V = \frac{V}{V_{box}} \tag{1}$$

  where V is the volume of the part and V_{box} is the volume of the bounding box.
- *detail index*, which measures the complexity of the part by taking into account the connected features by looking at the number of vertices and edges:

$$I_D = \frac{0.07}{\sqrt{N_v^2 + N_e^2}} \tag{2}$$

  where N_v is the number of vertices, N_e is the number of edges and the coefficient 0.07 is the value obtained for a conical part that has one vertex and one edge. I_D is assumed equal to 1 in the limit case of a spherical part.
- *freeform index*, which represents the complexity of the surfaces, measured in terms of the ratio of the number of freeform surfaces to the total number of surfaces (including regular surfaces):

$$I_F = 1 - \frac{N_{ff}}{N_{tot}} \tag{3}$$

  where N_{ff} is the number of freeform surfaces and N_{tot} is the total number of surfaces.

All three parameters are bounded between 0 and 1, values close to 0 suggest a complex geometry whereas values close to 1 a simple one. Therefore the complexity index (I_C) is defined as the sum of the three parameters, $I_C = I_V + I_D + I_F$. Whether I_C approaches 3, the geometry of the part becomes extremely simple. However, as the I_C approaches zero, the geometry becomes increasingly complex. From the perspective of sustainability, material waste is a key factor. Material waste considers all the accessory material that must be processed alongside the part, such as machining allowances, sprues and supports. A significant increase in material waste can lead to higher operational costs and broaden production times. In addition, surface finishing, usually expressed in terms of average

Figure 1. Methodology flow chart.

roughness, is relevant in ensuring high-quality parts. Low surface quality is detrimental not only for aesthetic reasons but also because it could reduce the corrosion resistance and the fatigue life of the part [28]. Finally, it is important to consider the energy required by the manufacturing process, particularly in the light of the current European GHG reduction plan [29]. The overall cost of the part should always be considered in process selection frameworks. A process that guarantees high technical performances at an enormous cost might not be convenient for all industrial sectors. Evaluating the time-to-market of a part can provide significant competitive advantages over competitors. Based on the above considerations, the criteria identified for this methodology are:

- Complexity index;
- Surface finishing;
- Material waste;
- Energy consumption;
- Time to market;
- Overall cost.

The relative weights of the aforementioned criteria are attributed by BWM, relatively new MCDM method proposed by Rezaei [13] in 2014. As opposed to previous MCDM methods such as the AHP method, BWM only compares alternatives with the best and worst ones, not in between them. In this manner, results reliability is improved, and number of comparisons to perform is minimised. The linear version of the BWM model Rezaei [30], easier to use and providing a unique solution, is implemented in the current study.

The final ranking of the alternative is provided by the PIV method. The PIV method is built on the pillar that the chosen option should be the one with the shortest distance from a fictitious best alternative [14]. The closeness to the best ideal solution is given by the overall proximity value computed during the process. Although this method seems close to the TOPSIS one, well known and established, it minimises the problem of rank reversal, strongly undesired in engineering applications [14]. PIV method allows to remove and/or add alternative to the ranking without meaningfully altering preference order yet defined.

The final ranking allows to identify the most suitable process for fabricating the component. In the event that AM is the best solution, the designer can apply the principles of DfAM and send the component design for engineerization. Otherwise, if AM did not result in the most promising manufacturing option, and if the complexity of the part is considered relatively low (complexity index greater than 1), an additional TO step might be considered. TO could suggest meaningful design changes to enhance the suitability of the component for AM, helping the user understanding if it is worth to invest time in more complex redesign activities. The implied hypothesis, already presented, is that a complex geometry holds a higher added value, making TO an appealing alternative. AM profitability could be increased by entry-level TO tools at this stage. After TO is performed, its result is again ranked by means of the MCDM method.

3. Case Study - Bracket for Aerospace Applications

The methodology described above was applied to a case study, a bracket for aerospace applications, the geometry of which was taken from the GrabCAD open library [31], and considered as a part concept (Figure 2). The bracket is a structural component, typically produced in AA2024 aluminium alloy by machining operations [32]. The AA2024 aluminium alloy is widely used in aircraft structures due to its high strength to weight ratio, good stiffness and corrosion resistance [33,34]. Moreover, the same AA2024 alloy has also been largely investigated in the scientific literature, providing a comprehensive knowledge on its processability [35,36]. The four holes on the base of the bracket allow its fastening to the underlying structure using bolted connections, whereas the through hole in the upper part of the bracket accommodates a rotating shaft, as schematically depicted in Figure 2. The tolerances and functional requirements of the part were determined using the Geometric Dimensioning and Tolerancing (GD&T) system, as outlined in UNI EN-ISO 22768 [37] (Figure 3). Tolerances of the order of the hundredth of a millimetre should be reached on

Table 1. Functional specifications.

Specification	Value
Maximum overall dimensions	$10 \times 10 \times 10\,mm^3$
Minimum wall thickness	5 mm
Maximum surface roughness, Ra	10 µm
Tolerances on mating surfaces	0.01 mm
General tolerances	ISO 2768-mK
Maximum weight	0.5 kg
Working load	4000 N
Minimum Safety Factor	1.5
Maximum deformation (magnitude)	0.5 mm

mating surfaces to ensure correct assembly. A production batch of 50 pieces is assumed. All bracket functional specifications were reported in Table 1.

3.1. Process Exploration

In alternative to CNC machining, the traditional high pressure die casting (HPDC) process and the powder bed fusion with laser beam and metallic powder (PBF-LB/M) were selected as candidate processes. The three alternatives were compared in an MCDM framework to define the best fitting solution. It is worth noting that both PBF-LB/M and HPDC processes will require additional machining operations, to reach the desired net shape and tolerances.

3.1.1. CNC Machining Process Exploration

Nowadays, machining processes such as drilling, turning and milling, represent a common route for processing complex-shaped aluminium components [38–40]. Limiting to the current case study, the selected AA2024 aluminium alloy, the dimensions of the bracket, its minimum wall thickness and the required surface quality do not represent an issue for part machinability, being well beneath the capability of commercial CNC machining centres. Only one enhancement was proposed to improve the machinability of the part concept, by increasing the minimum internal radius to 5 mm to avoid unnecessary finishing operations with custom tools. The refined design concept in AA2024 results in a mass of 0.260 kg, which is consistent with the specified limit. In order to evaluate the static response of the machined bracket and ascertain whether the maximum deformation is respected under the working load, Fusion 360, produced by Autodesk (San Francisco, CA, USA), was utilised. Fusion 360 was selected over other similar software packages primarily due to its relatively straightforward learning curve, which enables users to readily set up and launch structural analyses in an intuitive environment. In light of the fact that the intended user of the methodology is a technically-minded individual with limited experience of computer-aided engineering (CAE), the simplicity of the software package was identified as the primary factor to be taken into account. The resulting maximum deformation of 0.49 mm was below the set threshold of 0.5 mm (Figure 4). As result of this exploration, the CNC machining was considered eligible for the process selection phase. Updates to the product and process requirements for CNC machining are limited to increasing the minimum radius, as the part concept has been verified without any material changes.

3.1.2. High Pressure Die Casting Process Exploration

High pressure die casting is a widespread manufacturing process allowing the fabrication of complex shaped components at high production rate [41]. Aluminium, zinc and magnesium alloys are the most used materials, as excellent alloy castability is a mandatory prerequisite for a successful HPDC [41]. Although AA2024 exhibits excellent mechanical and corrosion resistance properties, it is not commonly casted, especially if complex shapes are required. Therefore, the ZL205A (AlCu5Mn) aluminium alloy was proposed as alternative material for the HPDC process. The ZL205A is an Al-Cu-Mn-Ti alloy already

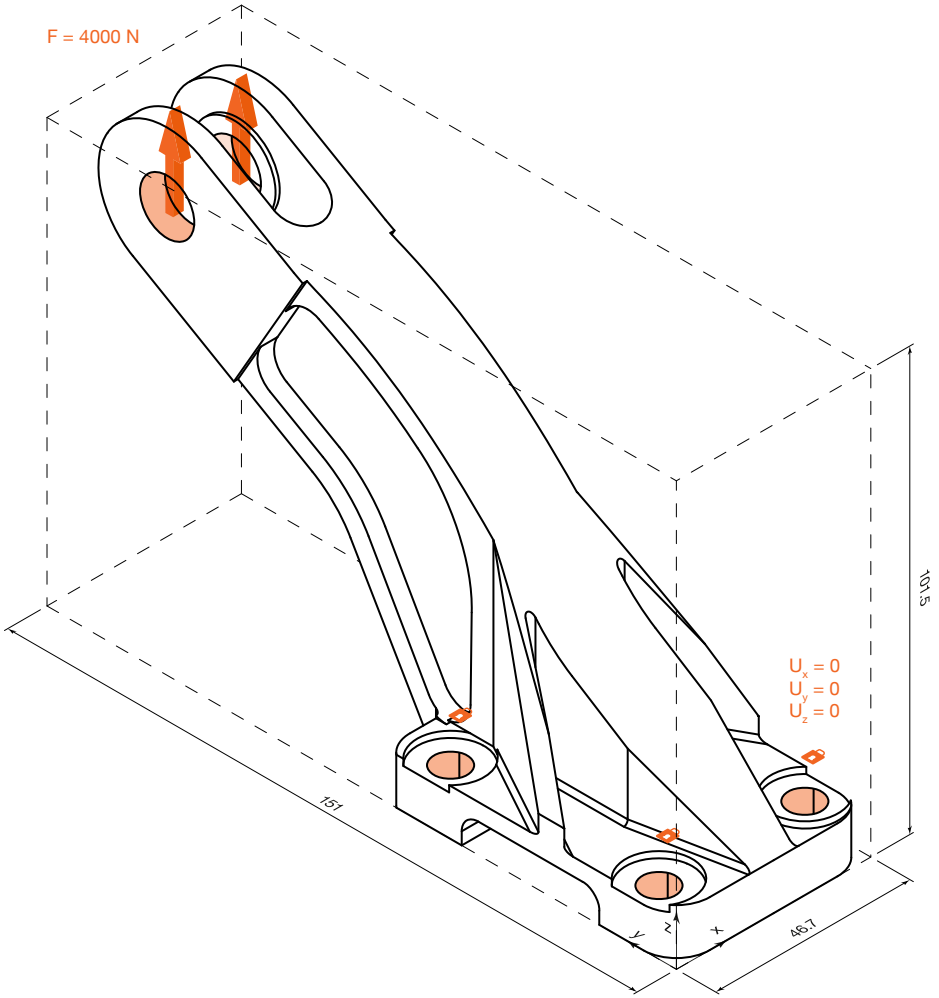

Figure 2. Isometric view of the aerospace bracket initial concept, mechanical loads and constraints highlighted. Bounding box represented as a dashed line.

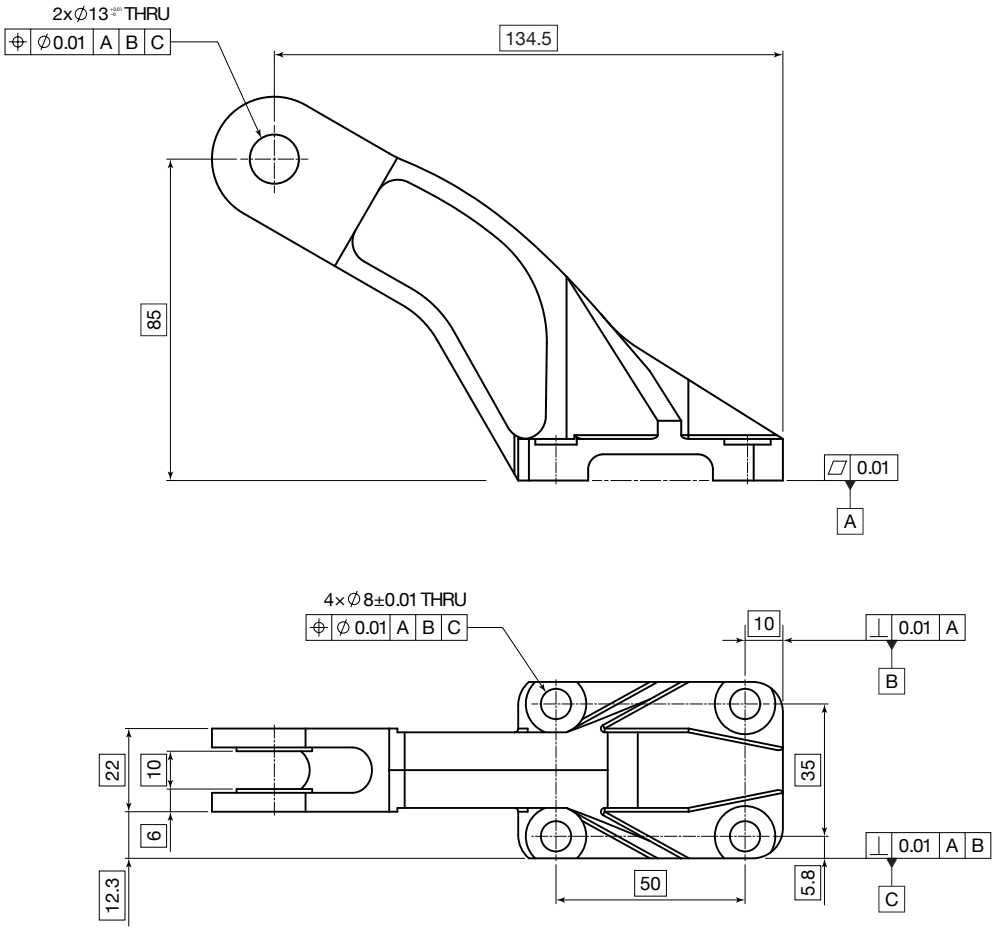

Figure 3. Dimensioned technical drawing of the aerospace bracket.

profitably used in casting operations for aircraft frame components [42–44]. The dimensions of the brackets were considered well inside the capabilities of HPDC systems, as well as its minimum wall thickness and surface quality. The minimum wall thickness producible by HPDC goes from 2 mm in the case of large castings, to 1 mm for smaller ones [45,46]. Wall thicknesses below this threshold may hinder the material flow resulting in unfilled voids in the mould cavity. Similarly, the presence of holes in the components should be carefully considered as they could induce vorticity in molten material, preventing a correct cavity filling. In light of the HPDC guidelines here synthetically exposed, the manufacturability of the concept of the bracket was asserted. However, some elements of the bracket might be easily modified to improve its manufacturability. In particular, the lateral ribs naturally create undercuts, requiring complex mould solutions with sensible higher costs. Therefore, they were removed from the part concept to allow for an easier processing. Moreover, the holes were also removed from the design considering that they can be easily produced in the subsequent CNC finishing operations. These refinements served to reduce the complexity of the geometry, allowing the part to be realised by orienting the larger dimension normal to the die closing, with only one undercut in correspondence with the fork of the bracket. The concept refinement is shown in Figure 4, together with the FE validation for maximum deformation, which resulted in a maximum deformation of 0.46 mm, which was below the set threshold of 0.5 mm. The mass of the parts is 0.262 kg also in this case. After this exploration, the HPDC bracket was finally considered eligible for the following process selection phase.

3.1.3. Additive Manufacturing | PBF-LB/M Process Exploration

Although PBF-LB/M systems allow the manufacture of extremely complex shapes [47], some basic limitations should be considered. The range of commercially available materials for PBF-LB/M is still very limited compared to conventional manufacturing processes. The original AA2024 alloy is not commercially available for PBF-LB/M systems, so a similar aluminium alloy had to be considered. A potential challenge in the proposed material substitution is the necessity to maintain the desired product performance. In this case study, the new material must meet the same functional specifications as the original. In particular, the bracket must adhere to the maximum deformation constraint under the working load, as outlined in Table 1. Aluminium alloys are largely used in the aerospace sector due to their lightweight and good mechanical performances [48]. However, there are alternative alloys that offer an excellent strength-to-weight ratio, such as titanium alloys, which are also suitable for use in aerospace applications [49]. Therefore, EOS Aluminium Al2139 AM, a 2000 series aluminium alloy developed specifically for AM [50], was chosen for its excellent mechanical and corrosion resistance properties. In addition to the aluminium alloy, a titanium alloy was also considered to widen the range of materials considered. Ti6Al4V was chosen because of its outstanding mechanical properties and widespread use in the manufacturing and aerospace industries [51].

The volume of commercial PBF-LB/M systems limits the maximum dimensions of the parts that can be manufactured, in order to avoid subsequent assembly operations. However, the part dimensions were well below the PBF-LB/M limits as shown in Appendix A. Similarly, the minimum wall thicknesses and overall features were considered feasible. As a rule of thumb, thin walls in PBF-LB/M should not be thinner than 1 mm to ensure their structural integrity, although recent studies have pushed the capabilities of commercial systems down to as little as 0.1 mm [52]. Finally, in addition to the simple feasibility of a part, its geometric accuracy and surface finish should also be considered, especially where tight tolerances are required. However, tolerances are not a critical factor when finishing operations follow the main manufacturing stage. In the case study analysed, the general tolerances are compatible with the AM process, considering that the mating surfaces require the finishing step of machining. Once the main limitations of PBF-LB/M systems have been outlined, the manufacturability of the specific bracket can be asserted. In conclusion, the bracket concept of PBF-LB/M was found to be feasible without the need for

Table 2. Best-to-others and Others-to-Worst vectors.

	Touchstone	Complexity Index	Surface finishing	Material waste	Energy consumption	Time to market	Overall cost
BO	Time to market	5	6	2	5	1	2
OW	Surface finish	2	1	4	2	7	5

design refinements, only a change in material. As previously stated, a change in material necessitates an evaluation of the performance of the product, ensuring that the specific functional requirements are fulfilled. Consequently, both brackets, the PBF-LB/Al2139 bracket and the PBF-LB/Ti6Al4V bracket, were subjected to a static verification process through numerical simulation. The PBF-LB/Al2139 bracket fulfilled the functional specifications with a maximum deformation of 0.43 mm (Figure 4), and a mass of 0.284 kg. The PBF-LB/Ti6Al4V option performed considerably better, with a maximum deformation of only 0.27 mm at a cost of a higher mass, equal to 0.444 kg.

3.2. Process Selection

Once the manufacturability of the part had been successfully stated for all the three process candidates, the MCDM method was applied. The first task was to define criteria weights using the BWM. The considered criteria are here recalled for the sake of simplicity: complexity index, surface finishing, material waste, energy required, time to market and overall cost. A reduced time to market allows a company to gain a competitive advantage with respect to other competitors. On the other hand, as-built surface roughness was expected to have a minor impact, especially when considering the need of machining operations in all manufacturing scenarios. Thus, for this case study the time to market was deemed the most important criterion, while the surface finishing was considered the least important. Table 2 reports the Best-to-Others (BO) and Others-to-Worst (OW) vectors, defined by comparison between touchstones and other criteria. Table 3 reports the final criteria weights computed following the rationale outlined in the Appendix B [52]. The consistency of criteria weights is demonstrated by the computed consistency ratio, equal to 0.052, being significantly close to zero.

Once the attribute weights were calculated, the decision matrix required by the PIV method was constructed by assigning to each candidate process a score for each attribute, as described in the following subsections.

3.2.1. Complexity index

The I_C of the refined concept was evaluated for each candidate process by using the three parameters introduced in Section 2, namely volumetric index (I_V), detail index (I_D), and freeform index (I_F). This evaluation is independent of the material. It only concerns the geometry. The AM bracket did not necessitate any alterations of the initial part concept. In this instance, the volume of the bracket was found to be 100 220 mm^3 whereas the volume of the parallelepiped bounding box of the component was 770 100 mm^3, resulting in a final I_V index of 0.130. The slight modification made on the CNC refined concept did not significantly alter the geometrical complexity, resulting approximately in the same I_V index of 0.130. The I_D index yielded for both AM and CNC concepts a relatively low value of only $5 \cdot 10^{-4}$, mostly due to the large number of vertices (110) and edges (80) of the model. Finally, the absence of freeform surfaces set the I_F index to one, which is its maximum value. The sum of the three parameters was therefore rounded to 1.131. Computations conducted on the HPDC bracket concept yielded slightly different indices, reflecting the concept refinement required by the same HPDC process. In particular, the I_V index was equal to 0.128, the I_D index equal to $8 \cdot 10^{-4}$, while the I_F index remained constant at one. As with previous calculations, the sum of the three indices was 1.129, rounded to the third decimal place.

Table 3. Criteria final weights.

Complexity index	Surface finishing	Material waste	Energy consumption	Time to market	Overall cost
0.083	0.052	0.208	0.083	0.365	0.208

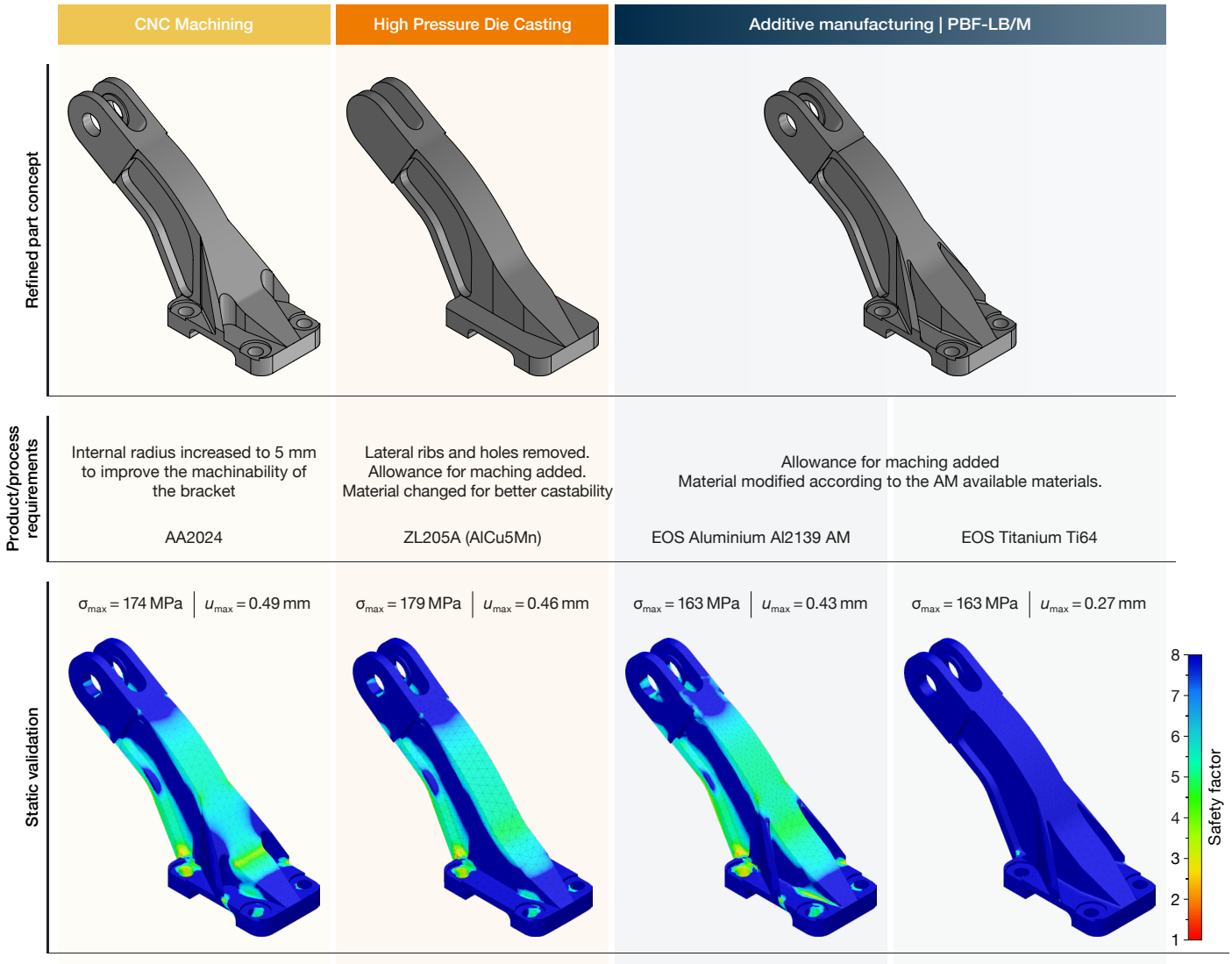

Figure 4. Concept refinements of the aerospace bracket, product requirements, and subsequent FE static validation. Coloured maps refer to the Safety Factor computed during static validation. Maximum stress and maximum deformation were reported for each refined concept.

3.2.2. Surface Finishing

Surface finishing, expressed in terms of average surface roughness, Ra, was estimated at 0.8 µm for machining operations on aluminium alloys, considering the final finishing machining step in the machining cycle. Ra was estimated at 1.5 µm for HPDC, value that can be easily reached with current HPDC systems [53,54]. The use of aluminium alloys allows for the achievement of a surface roughness of 10 µm Ra for PBF-LB/M, provided that the process parameters and shot peening are properly tuned [55,56]. In comparison, Ti6Al4V exhibits superior performance with an achievable surface roughness of 6 µm Ra.

3.2.3. Material Waste

CNC machining operations usually produce consistent amount of waste materials, typically in the shape of chips, being one of its major drawbacks when machining complex shapes. In the present case study, the volume of the waste material was computed as the difference between the volume of the parallelepiped bounding box surrounding the part and the part itself. Therefore, the resulting mass of waste material was found equal to 1.628 kg, slightly more than six times the mass of the bracket. HPDC usually requires the introduction of local allowances for subsequent finishing operations to achieve the required surface finish and geometric tolerances. In this case, a rule of thumb suggests to consider the allowance equal to the 10% of the mass of the component [57]. Given that the weight of the HPDC bracket was 0.260 kg, the corresponding allowance material was computed as 0.026 kg. PBF-LB/M accessory material consists of the allowances needed for subsequent finishing operations, as for HPDC operations, and the support structures required for the PBF-LB/M. Various approaches have been proposed to estimate the allowances required by AM processes [58,59]. In this work the approach proposed by Priarone, Ingarao [57] was chosen for computing the machining allowances, mainly due to its immediacy and simplicity, setting the allowance to 10% of the component weight. This resulted in 0.028 kg in the case of PBF-LB/Al2139 and in 0.044 kg in the case of PBF-LB/Ti6Al4V.

Additionally, supports volume was computed using Autodesk Netfabb Premium 2024, by Autodesk (San Francisco, CA, USA). The brackets were oriented and placed on a virtual representation of the building platform of the EOS M 290 system, by EOS GmbH (Krailing, Germany), in accordance with the standard orientation algorithm provided by Netfabb, trying to maximise the volume occupation. A total of 14 brackets were placed on a single platform, arranged as shown in Figure 5.

In accordance with the specified procedure, the fabrication of a single bracket necessitates the utilisation of a volume of 38 715 mm^3 of supports, resulting in an estimated mass of accessory material per bracket of 0.027 kg for PBF-LB/Al2139 and 0.043 kg for PBF-LB/Ti6Al4V, considering a support density of 25%. It is important to clarify why the supports were estimated using Netfabb rather than expressed as a simple fraction of the mass of the bracket. The introduction of a second software package is an inherent source of higher costs and longer training times for a company. However, Netfabb, as other commercially available software packages such as Magics by Materialize NV (Leuven, Belgium), allows the accurate definition of the number of parts to be fabricated at the same time, in what is commonly called "job". This piece of information is of utmost importance in the definition of manufacturing time, cost and energy required, and therefore cannot be overlooked.

3.2.4. Energy Consumption

The energy consumption of the three candidate processes was estimated considering only the process step and excluding the raw material production. It is important to differentiate the energy required by CNC machining when considering separately the parameters used for roughing and finishing operations. This is because the specific energy consumption (SEC) changes significantly from one condition to the other. Accordingly, the proportions of the total material removed during both machining phases must be established, along with the corresponding specific energy consumption. Priarone et al. [57] suggested that

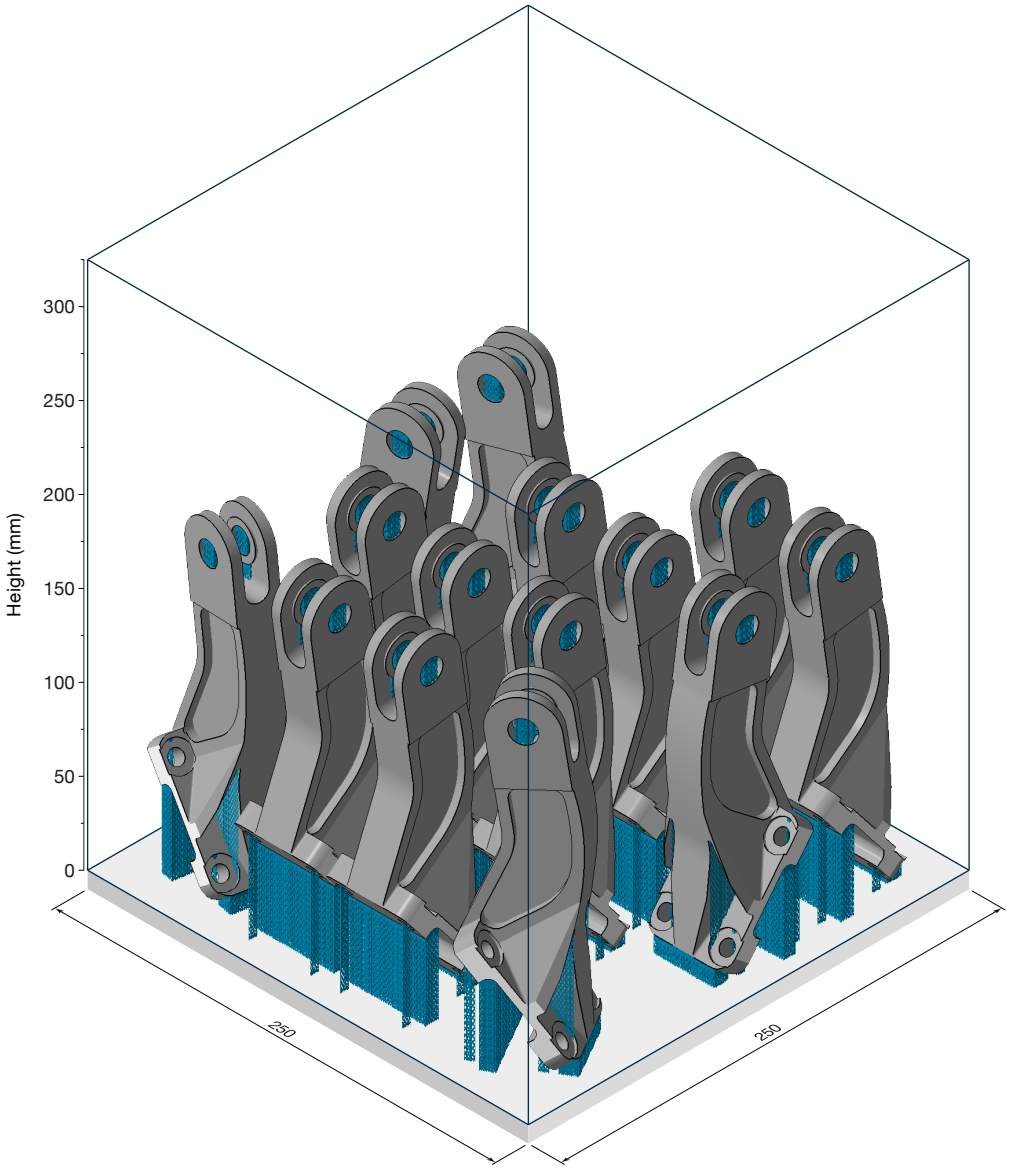

Figure 5. Proposed brackets orientations on the EOS M 290 building platform.

during the machining of aluminium alloys, 85% of the removed material occurs during rough machining, with the remaining 15% occurring during finishing operations. Ingarao et al. [60] also estimated the SECs of both rough machining and finishing operations of aluminium alloys to be 1.9 MJ · kg^{-1} and 6.8 MJ · kg^{-1} of removed material, respectively. This provides further evidence of the differing energy consumption of the two machining phases. Therefore, the overall energy required to produce the studied bracket by CNC machining was found equal to 4.7 MJ. Similarly, the energy consumption of HPDC was divided in energy used to melt and maintain the aluminium at high temperature, and the energy used by the actuators. Cecchel et al. [61] quantified the former energies using real foundry data, at 7 MJ · kg^{-1} and 1.5 MJ · kg^{-1} respectively, whereas Liu et al. [62] measured the energy required by all ancillary actuators to be approximately 0.8 MJ per working cycle. Overall, the energy required for the production of the HPDC bracket was found equal to 3.4 MJ. The subsequent finishing by machining of the allowance material, considering the same SEC of 6.8 MJ · kg^{-1}, accounted for 0.2 MJ. The energy required by the PBF-LB/M process was estimated using the average power consumption of the machine, assumed to be 2.4 kW [63]. The build time, t_{build}, was computed as:

$$t_{build} = \frac{V}{VR} + n \cdot t_{recoat} \tag{4}$$

where V is the aggregate volume of the job on the platform of the EOS M 290, VR is the volume rate allowed by the EOS M 290 machine for the two different materials that were taken into account, t_{recoat} is the time required to recoat a single layer (approximately 10 seconds on the EOS M 290 machine), and n is the number of layers required to complete the job. The volume rate of PBF-LB/Al2139 production is 7.2 mm^3 · s^{-1}, with a layer thickness of 60 µm [64]. In comparison, the volume rate of PBF-LB/Ti6Al4V is 5 mm^3 · s^{-1}, with a layer thickness of 30 µm [65]. A total of 2927 layers were required for PBF-LB/Al2139, with a total height of 175.6 mm, and 5853 layers were required for PBF-LB/Ti6Al4V. The build time for the PBF-LB/Al2139 job was found to be 83.2 hours, while the PBF-LB/Ti6Al4V job required 124.3 hours. The total build time for the single PBF-LB/Al2139 bracket was approximately 6 hours, while the PBF-LB/Ti6Al4V bracket required 8.9 hours. The values of 51.4 MJ and 76.7 MJ were found for the production of the PBF-LB/Al2139 bracket and the PBF-LB/Ti6Al4V bracket, respectively, which is generally in agreement with the high energy density of AM processes [60]. The energy consumption for the finishing operation was deemed negligible.

3.2.5. Time to Market

The time-to-market of the CNC machining bracket was estimated by the Xometry Europe (Ottobrunn, Germany) online service, together with its cost, and was equal to 14 working days. In contrast, the time-to-market for conventional high pressure die casting was estimated to be 30 working days, and to only one week for the PBF-LB/Al2139 and 10 days for the PBF-LB/Ti6Al4V bracket, stressing the different flexibility of these production systems. In fact, it is well-known that AM can help reducing the lead time of a part, enabling a quick response from the company, particularly when dealing with small batches [66,67], thus justifying the shortest time-to-market out of the three processes. It is worth noting that the considered time-to-market for HPDC and PBF-LB/M include the consideration of the final finishing.

3.2.6. Overall Cost

The cost of CNC machining operations was estimated using the online free tool offered by Xometry Europe. The online service provided by Xometry carefully considered the 3D CAD model of the bracket, its material and the expected resulting surface roughness, enhancing the accuracy of the final estimate. Therefore, a cost of 95 € per bracket was computed this way. As for HPDC, the higher complexity hindered by the process did not allow the use of any online tool for cost estimation, nudging the authors to opt for

Table 4. Decision matrix.

	Complexity index (-)	Surface finishing (µm)	Material waste (kg)	Energy consumption (MJ)	Time to market (working days)	Overall cost (€)
CNC Machining	1.131	0.8	1.628	4.7	14	96
HPDC	1.129	1.5	0.026	3.6	30	659
PBF-LB/Al2139	1.131	10	0.055	51.4	7	812
PBF-LB/Ti6Al4V	1.131	6	0.087	76.7	10	1348

Table 5. Normalised decision matrix.

	Complexity index	Surface finishing	Material waste	Energy consumption	Time to market	Overall cost
CNC Machining	0.500	0.068	0.998	0.051	0.397	0.056
HPDC	0.499	0.127	0.016	0.039	0.850	0.286
PBF-LB/Al2139	0.500	0.849	0.034	0.556	0.198	0.475
PBF-LB/Ti6Al4V	0.500	0.509	0.053	0.829	0.283	0.789

empirical models to estimate the cost of the bracket. It this scenario, the model developed by Atzeni and Salmi [68] was referenced for the cost evaluation of the HPDC bracket. While reporting the whole breakdown structure of the model would go beyond the scope of this investigation, it is worth noticing some of the assumption made. The overall cost was divided into four items: material cost per part, machine setup cost, machine operation cost and post-processing costs. Assuming a die cost of roughly 30 000 €, for a batch of 50 pieces the price per bracket would be near 659 €, as reported in the respective column of Table 4. The same study was also considered when estimating the cost of the PBF-LB/M bracket. Also in this case the total cost per bracket was divided in the same four cost items: material cost per part, machine setup cost, processing cost and post-processing costs. The model resulted in a cost of 812 € per the PBF-LB/Al2139 bracket and 1348 € per the PBF-LB/Ti6Al4V bracket, with the machine cost accounting for over than 85% of the total value. Table 4 presents all data collected in this section and organises them for an easier implementation of the following hybrid MCDM methodology.

The decision matrix was then normalised to enable comparison of different scores. Every element of the matrix was normalised by dividing it by the square root of the sum of squares of the corresponding column, resulting in a dimensionless number. Table 5 presents the normalised data for the batch of 50 pieces. Each column entry was then multiplied by the corresponding weight to generate the weighted normalised decision matrix, as shown in Table 6. From the weighted normalised decision matrix the ideal best, Positive Ideal Solution (PIS), was computed by selecting the smallest options for each attribute in each column, as all attributes were considered costs. PIS components are reported in the last row of the same Table 6.

Table 6. Weighted normalised decision matrix.

	Complexity index	Surface finishing	Material waste	Energy consumption	Time to market	Overall cost
CNC Machining	0.042	0.004	0.208	0.004	0.145	0.012
HPDC	0.042	0.007	0.003	0.003	0.310	0.080
PBF-LB/Al2139	0.042	0.044	0.007	0.046	0.072	0.099
PBF-LB/Ti6Al4V	0.042	0.027	0.011	0.069	0.103	0.164
Ideal best (PIS)	0.042	0.004	0.003	0.003	0.072	0.012

Table 7. PIV of the explored manufacturing processes.

	PIV	Rank
CNC machining	0.278	2
HPDC	0.310	4
PBF-LB/Al2139	**0.175**	**1**
PBF-LB/Ti6Al4V	0.280	3

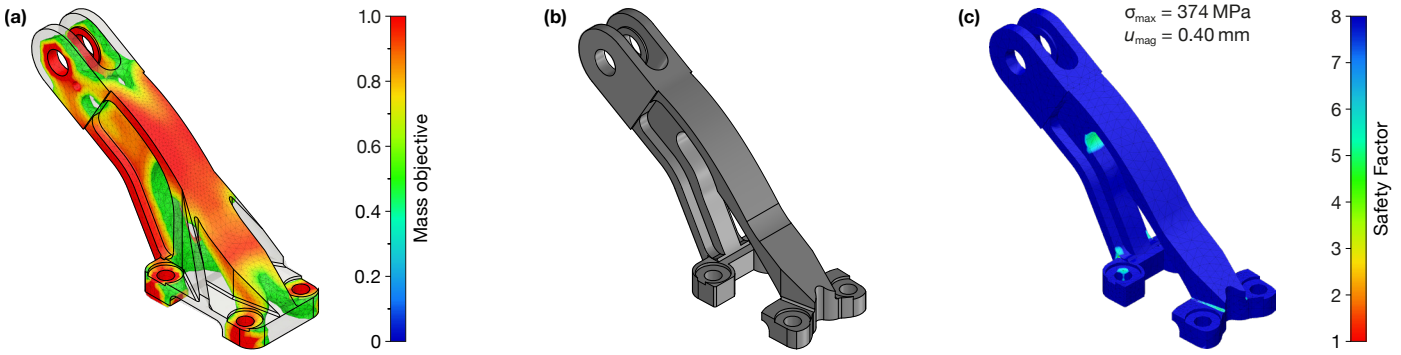

Figure 6. (**a**) TO results. (**b**) Redesigned bracket. (**c**) FE validation of the redesigned bracket.

The overall proximity index values, PIV, of the three processes is equal to the Manhattan distance between the ideal best solution and the solutions provided by the same manufacturing processes. PIV is reported in Table 7. It is worth recalling that a lower PIV suggests a closer solution to the ideal best, and therefore a most suitable solution. Thus, PBF-LB/Al2139 resulted as the most suitable process for the production of the considered bracket. The same procedure deemed less suitable both the CNC machining and the PBF-LB/Ti6Al4V, which both resulted in very close PIVs. Finally, the HPDC was found to be the least adequate option out the investigated four. At this stage, the proposed methodology highlighted the profitability of PBF-LB/M for the production of a bracket for aerospace applications, both in aluminium and titanium alloys, and low production batch.

3.3. Other Scenarios

It is therefore evident that the choice of the right material can severely influence the results of the whole hybrid MCDM method. Ti6Al4V has considerable higher mechanical properties than Al2139, together with a considerably higher density. Using Ti6Al4V as an alternative to aluminium alloys, without coherently change the concept of the same bracket, may partially hinder the potentialities of the material. Therefore, given that the I_C is greater than unity, it might be beneficial to explore the potential of utilising an inspiring TO to reduce the mass of the titanium bracket, thereby enhancing its suitability for the production by PBF-LB/M and improving its score at the end of the MCDM method.

3.3.1. Topology Optimisation

The TO step was completed within the Fusion 360 simulation environment, without the necessity for additional software packages. Figure 6a depicts the outcomes of the TO, highlighting the difference between the initial design and the optimal solution proposed by Fusion 360. The redesigned bracket concept was considerably less bulky than the original one (Figure 6b) with a substantial lower mass that was reduced from the original 0.444 kg to 0.273 kg, marking a 39% reduction. The optimised concept was also positively tested for the initial functional specifications. The maximum displacement computed was equal to 0.40 mm, which is below the threshold of 0.5 mm (Figure 6c), and therefore considered eligible for process selection.

It was found that the modifications made to the titanium bracket geometry had an appreciable influence on the MCDM analysis. Computations were performed to determine

Table 8. Decision matrix after TO.

	Complexity index (-)	Surface finishing (µm)	Material waste (kg)	Energy consumption (MJ)	Time to market (working days)	Overall cost (€)
CNC Machining	1.131	0.8	1.628	4.7	14	96
HPDC	1.129	1.5	0.026	3.6	30	659
PBF-LB/Al2139	1.131	10	0.055	51.4	7	812
PBF-LB/Ti6Al4V | After TO	1.076	6	0.090	72.8	10	1155

Table 9. PIVs after TO.

	PIV	Rank
CNC machining	0.278	3
HPDC	0.316	4
PBF-LB/Al2139	**0.184**	**1**
PBF-LB/Ti6Al4V	0.267	2

the new I_V and I_D indices, which yielded an I_C of 1.076. The reduction in the allowance, which is directly proportional to the part weight, was offset by the greater necessity for supports, resulting in a final value of 0.090 kg of material waste per bracket. The most consistent changes, which also had the greatest impact on the final process ranking, were related to the overall cost of the bracket and to its energy consumption. The reduction in bracket mass following the TO stage resulted in a decrease in manufacturing time, which in turn led to a reduction in energy consumption, amounting to 72.8 MJ in this scenario. Similarly, the overall cost was reduced to 1155 €, resulting in savings of €193 per bracket. Table 8 represents the decision matrix updated to consider the PBF-LB/Ti6Al4V bracket after the TO. The incorporation of the novel values in Table 8 resulted in a considerably different final ranking, as reported in Table 9. The PBF-LB/Ti6Al4V process emerged as the second most suitable option, distinguishing itself from the CNC machining process and deepening the distance from the HPDC one.

3.3.2. Production Batch Sensibility

However, the outcomes yielded by the proposed hybrid MCDM method were found to be significantly influenced by the dimensions of the production batch. To assess the impact of varying the batch size, the batch was divided by two, multiplied by two, and multiplied by 20. A further MCDM analysis was conducted for these scenarios. Although smaller batches do not appear to significantly impact the prioritisation of the selected processes (Figure 7), differences were introduced by scenarios of larger batches. In fact, the production batch of 100 pieces was sufficiently large to significantly reduce the cost of a single bracket produced by HPDC, down to 359 €. This made the HPDC the second-best option, surpassing both the CNC machining solution and the PBF-LB/Ti6Al4V solution. Furthermore, the cost of the HPDC bracket was markedly reduced for the largest production batch considered, comprising 1000 pieces, reaching only 89 € per piece. This sharp decline in production costs was reflected in the significantly lower PIV of the HPDC, creating a substantial margin separating the HPDC from the PBF-LB/Ti6Al4V solution. It is evident that this trend would eventually position the HPDC as the most viable option for larger production volumes, even when compared to the PBF-LB/Al2139 solution.

4. Conclusions

The present investigation proposed a methodology aimed at choosing the best manufacturing process for a specific scenario, with special attention on the distinction between AM and conventional processes. The methodology was evaluated on a case study taken

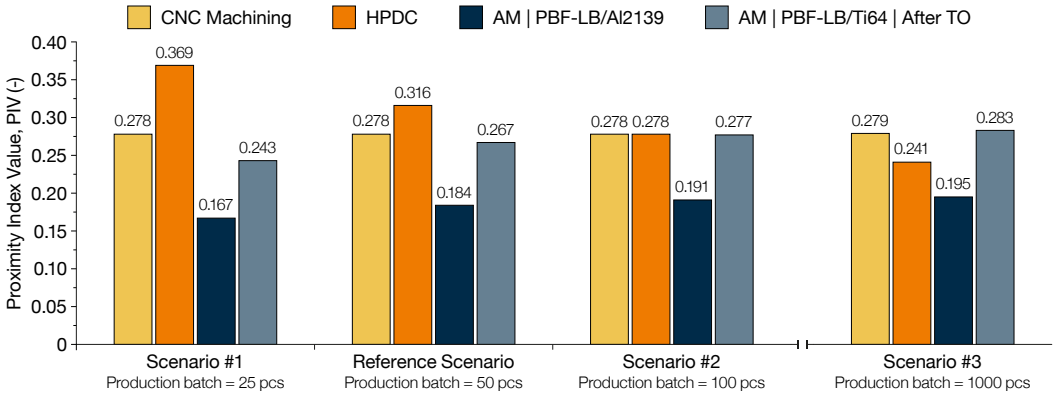

Figure 7. PIV of CNC machining, HPDC and PBF-LB/M as a function of batch number.

from the aeronautical field to show the proficiency of the entire proposed workflow. The main results of the investigation can be summarised as follows:

- The methodology put forth a hybrid MCDM approach to evaluate the relative suitability of AM and CM processes, which can be readily utilised by technical professionals without a strong background in AM.
- AM processes were found to be ideal for the production of small to medium batches, up to 100 pieces, leveraging their higher flexibility due to the absence of initial tooling costs.
- The significance of material selection in the context of AM during the preliminary design phase was emphasised. In fact, the utilisation of materials with a high strength-to-weight ratio, such as titanium alloys, necessitated supplementary redesign activities to enhance the suitability of AM techniques in comparison to conventional ones.
- In the context of redesign activities, it was confirmed the positive role that TO may cover. The implementation of TO resulted in a 39% reduction in the weight of the bracket, thereby positively influencing the manufacturing time. The reduction in manufacturing time subsequently resulted in a 10% improvement in terms of cost and 5% improvement for energy consumption, which in turn enhanced the score of AM in the final process ranking.
- The use of CM techniques, such as HPDC, has been demonstrated to offer a highly competitive solution for the production of large batches, larger than 100 pieces, where the initial tooling costs associated with the mould can be distributed across a greater number of components.

In conclusion, the human role in the production planning is still central and high skilled work figures must still rely on their experience while incorporating multiple elements during their decision-making processes. Nonetheless, the methodology proposed can help newcomers, and less skilled workers, to still take a reliable decision thanks to a guided and robust procedure. Future works might go even further in this same direction, trying to use artificial intelligence algorithms in the decision making process.

Author Contributions: Conceptualization, A.S, E.A., and L.I.; methodology, G.V.; validation, G.V.; investigation, G.V.; resources, A.S, E.A., and L.I.; writing—original draft preparation, G.V.; writing—review and editing, A.S, G.V., E.A., and L.I.; visualization, A.S. and G.V. All authors have read and agreed to the published version of the manuscript.

Funding: This research received no external funding.

Acknowledgments: The authors would like to acknowledge the Interdepartmental Centre for Integrated Additive Manufacturing (IAM@PoliTo) at the Politecnico di Torino, Torino, Italy, for the resources to perform the research activities.

Conflicts of Interest: The authors declare no conflict of interest.

Abbreviations

The following abbreviations are used in this manuscript:

AM	Additive Manufacturing
AHP	Analytic Hierarchy Process
BO	Best-to-Others
BWM	Best Worst Method
CAD	Computer-Aided Design
CAE	Computer-Aided Engineering
CM	Conventional Manufacturing
CNC	Computer Numerically Controlled
DfAM	Design for Additive Manufacturing
FDM	Fused Deposition Modeling
FE	Finite Element
FGM	Fuzzy Geometric Mean
GD&T	Geometric Dimensioning and Tolerancing
GHG	Greenhouse Gases
HPDC	High Pressure Die Casting
MCDM	Multi-Criteria Decision-Making
OW	Others-to-Worst
PBF-LB	Powder Bed Fusion with Laser Beam
PIS	Positive Ideal Solution
PIV	Proximity Index Value
RP	Rapid Prototyping
SEC	Specific Energy Consumption
TO	Topology Optimization
TOPSIS	Technique for Order of Preference by Similarity to Ideal Solution
VIKOR	VIekriterijumsko KOmpromisno Rangiranje
WPI	Weighted Proximity Index

Appendix A Building Volumes and Available Materials of AM Commercial Systems

In this first appendix the volumes of commercially available AM systems have been reported. Ensuring a building volume large enough to accommodate the whole component in production is a key feature of AM systems, avoiding the need of subsequent assembly operations. Table A1 contains the building volume dimensions of some of the most common commercial systems [69]. Similarly, designers must consider the plethora of commercially available AM materials during the initial design phases. Later material changes might require undesired concept changes to respect functional specifications. Table A2 reports some of the most used materials in PBF-LB/M applications.

Appendix B BWM and PIV Rationales

This appendix presents the rationales behind the BWM and the PIV method used in this investigation. The BWM was used to define the weights of the criteria considered, whereas the PIV method was used to rank the manufacturing processes. As already explained, the BWM was introduced to reduce the number of pair-wise comparisons between different options, improving the consistency of the results obtained [13,30]. The BWM is carried out as follows:

1. Definition of the set of criteria to compare.
2. Select the best criterion and the worst criterion in the current scenario. Only primary comparisons are carried out, namely between the best criterion and the other options, and between the worst criterion and the other options. This way all the so-called secondary comparisons can be avoided, drastically reducing the number of comparisons.
3. Define the best-to-others vector, whose components quantify how much the best criterion is preferred over the others. The value 1 indicates the same importance

Table A1. PBF-LB/M commercially available systems.

Company	**Model Name**	**X** (mm)	**Y** (mm)	**Z** (mm)	Ref.
3D SYSTEMS	DMP Flex 200	140	140	115	[70]
	DMP Factory 350	275	275	420	[71]
	DMP Factory 350 Dual	275	275	420	[71]
	DMP Flex 350	275	275	420	[72]
	DMP Flex 350 Dual	275	275	420	[72]
	DMP Flex 350 Triple	275	275	420	[72]
	DMP Factory 500	500	500	500	[73]
Colibrium Additive	M2 Series 5	245	245	350	[74]
	M Line	500	500	400	[75]
	X Line 2000R	800	400	500	[76]
DMG MORI	Lasertec 12 SLM	125	125	200	[77]
	Lasertec 30 Dual SLM	300	300	300	[78]
EOS	M 290	250	250	325	[63]
	M 300-4	300	300	400	[79]
	M 400	400	400	400	[80]
	M 400-4	400	400	400	[81]
Farsoon Technologies	FS121M	120	120	100	[82]
	FS273M	275	275	355	[83]
	FS200M	425	230	300	[84]
	FS301M	305	305	410	[85]
	FS350M-4	433	358	400	[86]
	FS422M	425	425	550	[87]
	FS721M-CAMS	720	420	390	[88]
	FS721M	720	420	420	[89]
	FS621M	620	620	1100	[90]
Matsuura Machinery	LUMEX Avance-25	256	256	300	[91]
	LUMEX Avance-60	600	600	500	[92]
Prima Additive	Print Sharp 150		Φ150	160	[93]
	Print Genius 150		Φ150	160	[94]
	Print Green		Φ150	160	[95]
	Print Sharp 300	330	330	400	[96]
	Print Genius 300	330	330	400	[96]
	Print Brilliance 300	330	330	400	[96]
	Print Genius 400	430	430	600	[97]
	Print Genius 400 XL	430	430	1000	[97]
Renishaw	RenAm 500 Flex	250	250	350	[98]
	RenAM 500	250	250	350	[98]
	RenAM 500 Ultra	250	250	350	[98]
SLM Solutions	SLM 125	125	125	125	[99]
	SLM 280 PS	280	280	365	[100]
	SLM 280 2.0	280	280	365	[101]
	SLM 500	500	280	365	[102]
	SLM 800	500	280	850	[103]
	SLM NXG XII 600	600	600	600	[104]
Sharebot	metalONE	65	65	100	[105]
TRUMPF	TruPrint 1000		Φ 100	100	[106]
	TruPrint 1000 Basic Edition		Φ 100	100	[107]
	TruPrint 2000	200	200	200	[108]
	TruPrint 3000		Φ 300	400	[109]
	TruPrint 5000		Φ 300	400	[110]
	TruPrint 5000 Green Edition		Φ 300	400	[111]
Velo3D	Sapphire		ϕ 315	400	[112]
	Sapphire 1MZ		315	1000	[112]
	Sapphire XC		600	550	[113]
	Sapphire XC 1MZ		600	1000	[113]

Table A2. PBF-LB/M commercially available materials.

Material class	Alloy	Providers
Aluminium	Aheadd® CP1	3D SYSTEMS
	Al-HS1®	Höganäs
	AlSi7Mg0.6	3D SYSTEMS, Colibrium Additive, EOS, SLM Solutions
	AlSi10Mg	3D SYSTEMS, Colibrium Additive, EOS, Farsoon Technologies, Prima Additive, SLM Solutions, Höganäs
	AlSi12	3D SYSTEMS
	Al2139	EOS
Cobalt-Chrome	CoCrF75	3D SYSTEMS
	CoCrMo	3D SYSTEMS, Colibrium Additive, EOS, Farsoon Technologies, Prima Additive, Höganäs
	CoCrMoW	Farsoon Technologies, Prima Additive
	SLM MediDent®	SLM Solutions
Copper	Oxygen-Free Copper	3D SYSTEMS, EOS, Prima Additive
	CuCr1Zr	3D SYSTEMS, EOS, SLM Solutions, Höganäs
	GRCop-42	3D SYSTEMS
	CuCr2.4	3D SYSTEMS
	CuNi2SiCr	SLM Solutions
	CuNi30	3D SYSTEMS, EOS
	CuSn10	Farsoon Technologies, Prima Additive
Nickel	HAYNES® 282®	EOS, Höganäs
	GRX-810	3D SYSTEMS
	HX	3D SYSTEMS, EOS, Farsoon Technologies, Prima Additive, SLM Solutions, Höganäs, Oerlikon
	K-500	SLM Solutions
	IN625	3D SYSTEMS, Colibrium Additive, EOS, Farsoon Technologies, Prima Additive, SLM Solutions, Höganäs, Oerlikon
	IN718	3D SYSTEMS, Colibrium Additive, EOS, Farsoon Technologies, Prima Additive, SLM Solutions, Höganäs, Oerlikon
	IN939	EOS, Höganäs
Refractory	C-103	3D SYSTEMS
	Tungsten	3D SYSTEMS
Steel	Invar 36®	SLM Solutions
	M300	3D SYSTEMS, Colibrium Additive, EOS, Farsoon Technologies, Prima Additive
	Tool Steel H11	Höganäs, Oerlikon
	Tool Steel H13	EOS, SLM Solutions, Höganäs, Oerlikon
	316L	3D SYSTEMS, Colibrium Additive, EOS, Farsoon Technologies, Prima Additive, SLM Solutions, Höganäs, Oerlikon
	17-4PH	3D SYSTEMS, Colibrium Additive, EOS, Farsoon Technologies, Prima Additive, SLM Solutions, Höganäs, Oerlikon
	15-5PH	Farsoon Technologies, SLM Solutions, Oerlikon
Titanium	TA15	Farsoon Technologies, SLM Solutions
	CPTi grade 1	3D SYSTEMS, Colibrium Additive
	CPTi grade 2	Colibrium Additive, EOS, SLM Solutions, Höganäs
	Ti6Al4V grade 5	3D SYSTEMS, Colibrium Additive, EOS, Farsoon Technologies, Prima Additive, Höganäs, Oerlikon
	Ti6Al4V grade 23	3D SYSTEMS, Colibrium Additive, EOS, SLM Solutions, Höganäs, Oerlikon
	Ti-6Al-2Sn-4Zr-2Mo	Colibrium Additive
	Ti-5Al-5V-5Mo-3Cr	Colibrium Additive

between criteria, while the value 9 indicates the utmost importance of the best criterion over the second one.

$$A_B = (a_{B1}, a_{B2}, \ldots, a_{Bn}) \tag{A1}$$

4. Define the others-to-worst vector, following the same procedure explained at the previous step. As before, the value 1 indicates the same importance between the criteria, whereas 9 a prominent importance of the others over the worst criterion.

$$A_W = (a_{1W}, a_{2W}, \ldots, a_{nW})^T \tag{A2}$$

5. Defining the vector of the optimal weight w^*, as $w^* = (w_1^*, w_2^*, \ldots, w_n^*)$ for which the differences $|w_B/w_j - a_{Bj}|$ and $|w_j/w_W - a_{jW}|$ are minimised for all j, namely for all the components of the w vector.

The problem can be formulated as finding the minimum value of ξ so that:

$$\begin{cases} \left| \dfrac{w_B}{w_j} - a_{Bj} \right| < \xi \\ \left| \dfrac{w_j}{w_W} - a_{jW} \right| < \xi \\ \sum_j w_j = 1, w_j > 0 \forall j \end{cases} \tag{A3}$$

The smallest ξ granting a non-empty solution space is called ξ^* and defines the optimal weight vector w^*.

The PIV method was firstly introduced to overcome the rank reversal phenomenon often occurring in the TOPSIS method [14]. The rationale behind the PIV method is quite close with the TOPSIS one, with slight differences in the final part of the procedure. The PIV method may be schematically presented as a seven steps procedure:

1. Formulation of the decision problems by defining decision criteria $C_J(j = 1, \ldots, n)$ and alternatives, $A_i(i = 1, \ldots, m)$.
2. Each alternative is evaluated on every criteria, resulting in a score x_{ij}. The x_{ij} scores constitute the decision matrix (DM), as shown in Table A3.
3. The scores x_{ij} are likely to be expressed in various unit of measures, making it difficult to directly compare them. The normalisation step solves this problem, bringing all x_{ij} to a common scale. The normalised entry of the decision matrix, r_{ij}, is computed as $r_{ij} = x_{ij}/\sqrt{\sum_{i=1}^{m} x_j^2}$.
4. After the definition of the normalised decision matrix, each r_{ij} must be multiplied by the corresponding w_j weight, defined in advance. Therefore, the weighted entries of the decision matrix are defined as $v_{ij} = w_j \cdot r_i$, as in Table A4.
5. The weighted proximity index (WPI) expresses the distance between each alternative and the ideal best alternative. If the criterion expresses a benefit for the alternatives, the ideal best components is the v_i scoring the highest value along the column. Conversely, if the criterion expresses a cost for the alternative, the ideal best components is represented by the lowest v_i along the column. The components of the WPI, namely u_i, are computed as $u_i = |v_{best} - v_i|$. This step represents the key moment of the whole procedure, distinguishing the PIV method from the TOPSIS one. In fact, the use of the 1-norm, instead of the Euclidean norm used by the TOPSIS method, should minimise the occurring of the rank reversal.
6. The 1-norm distances between alternative components and ideal best can be summed up into the overall proximity value (d_j), expressing the closeness of the alternative to the ideal best, namely $d_i = \sum_{j=1}^{n} u_j$.
7. In conclusion, the alternatives can be ranked according to their overall proximity value, from the smallest to the highest one.

Table A3. Decision matrix.

	w_1 C_1	w_2 C_2	... ...	w_n C_n
A_1	x_{11}	x_{12}	...	x_{1n}
A_2	x_{21}	x_{22}	...	x_{2n}
$\vdots$	$\vdots$	$\vdots$	$\ddots$	$\vdots$
A_m	x_{m1}	x_{m2}	...	x_{mn}

Table A4. Weighted normalised decision matrix.

	w_1 C_1	w_2 C_2	... ...	w_n C_n
A_1	v_{11}	v_{12}	...	v_{1n}
A_2	v_{21}	v_{22}	...	v_{2n}
$\vdots$	$\vdots$	$\vdots$	$\ddots$	$\vdots$
A_m	v_{m1}	v_{m2}	...	v_{mn}

References

1. Dieter, G.E.; Schmidt, L.C. *Engineering design*, 4th ed.; McGraw-Hill Higher Education: New York, 2009.
2. ASTM International, West Conshohocken, PA. *Additive manufacturing — General principles — Fundamentals and vocabulary*, 2021. Available online: https://www.astm.org/f3177-21.htm (accessed on 05-08-2024).
3. Wohlers, T.; Gornet, T. History of additive manufacturing. Wholers Report 2016, 2016. Available online: https://wohlersassociates.com/product/wohlers-report-2016/ (accessed on 01-06-2024).
4. Salmi, A.; Calignano, F.; Galati, M.; Atzeni, E. An integrated design methodology for components produced by laser powder bed fusion (L-PBF) process. *Virtual and Physical Prototyping* **2018**, *13*, 191–202. https://doi.org/10.1080/17452759.2018.1442229.
5. Jared, B.H.; Aguilo, M.A.; Beghini, L.L.; Boyce, B.L.; Clark, B.W.; Cook, A.; Kaehr, B.J.; Robbins, J. Additive manufacturing: Toward holistic design. *Scripta Materialia* **2017**, *135*, 141–147. https://doi.org/10.1016/j.scriptamat.2017.02.029.
6. Zhai, Y.; Lados, D.; LaGoy, J. Manufacturing: Making Imagination the Major Limitation. *JOM* **2014**, *66*, 808–816. https://doi.org/10.1007/s11837-014-0886-2.
7. Fayazfar, H.; Sharifi, J.; Keshavarz, M.K.; Ansari, M. An overview of surface roughness enhancement of additively manufactured metal parts: a path towards removing the post-print bottleneck for complex geometries. *The International Journal of Advanced Manufacturing Technology* **2023**, *125*, 1061–1113. https://doi.org/10.1007/s00170-023-10814-6.
8. Piscopo, G.; Salmi, A.; Atzeni, E. Investigation of dimensional and geometrical tolerances of laser powder directed energy deposition process. *Precision Engineering* **2024**, *85*, 217–225. https://doi.org/10.1016/j.precisioneng.2023.10.006.
9. Yang, S.; Page, T.; Zhang, Y.; Zhao, Y.F. Towards an automated decision support system for the identification of additive manufacturing part candidates. *Journal of Intelligent Manufacturing* **2020**, *31*, 1917–1933. https://doi.org/10.1007/s10845-020-01545-6.
10. Taherdoost, H.; Madanchian, M. Multi-Criteria Decision Making (MCDM) Methods and Concepts. *Encyclopedia* **2023**, *3*, 77–87. https://doi.org/10.3390/encyclopedia3010006.
11. Velasquez, M.; Hester, P.T. An analysis of multi-criteria decision making methods. *International journal of operations research* **2013**, *10*, 56–66.
12. Qin, Y.; Qi, Q.; Shi, P.; Lou, S.; Scott, P.J.; Jiang, X. Multi-Attribute Decision-Making Methods in Additive Manufacturing: The State of the Art, 2023. https://doi.org/10.3390/pr11020497.
13. Rezaei, J. Best-worst multi-criteria decision-making method: Some properties and a linear model. *Omega* **2016**, *64*, 126–130. https://doi.org/10.1016/j.omega.2015.12.001.
14. Mufazzal, S.; Muzakkir, S.M. A new multi-criterion decision making (MCDM) method based on proximity indexed value for minimizing rank reversals. *Computers & Industrial Engineering* **2018**, *119*, 427–438. https://doi.org/10.1016/j.cie.2018.03.045.
15. Qin, Y.; Qi, Q.; Shi, P.; Scott, P.J.; Jiang, X. Selection of materials in metal additive manufacturing via three-way decision-making. *The International Journal of Advanced Manufacturing Technology* **2023**, *126*, 1293–1302. https://doi.org/10.1007/s00170-023-10966-5.
16. Jayapal, J.; Kumaraguru, S.; Varadarajan, S. Evaluation of computationally optimized design variants for additive manufacturing using a fuzzy multi-criterion decision-making approach. *The International Journal of Advanced Manufacturing Technology* **2023**, *129*, 5199–5218. https://doi.org/10.1007/s00170-023-12641-1.
17. Sakthivel Murugan, R.; Vinodh, S. Prioritization and deployment of design for additive manufacturing strategies to an automotive component. *Rapid Prototyping Journal* **2023**, *29*, 2193–2215. https://doi.org/10.1108/RPJ-02-2023-0051.

18. Sartini, M.; Luca, M.; Claudio, F.; Marco, M. A MULTI-CRITERIA DECISION-MAKING APPROACH TO OPTIMIZE THE PART BUILD ORIENTATION IN ADDITIVE MANUFACTURING. *Proceedings of the Design Society* **2023**, *3*, 293–302. https://doi.org/10.1017/pds.2023.30.
19. Mançanares, C.G.; de S. Zancul, E.; Cavalcante da Silva, J.; Cauchick Miguel, P.A. Additive manufacturing process selection based on parts' selection criteria. *The International Journal of Advanced Manufacturing Technology* **2015**, *80*, 1007–1014. https://doi.org/10.1007/s00170-015-7092-4.
20. Liu, W.; Zhu, Z.; Ye, S. A decision-making methodology integrated in product design for additive manufacturing process selection. *Rapid Prototyping Journal* **2020**, *26*, 895–909. https://doi.org/10.1108/rpj-06-2019-0174.
21. Zaman, U.K.u.; Rivette, M.; Siadat, A.; Mousavi, S.M. Integrated product-process design: Material and manufacturing process selection for additive manufacturing using multi-criteria decision making. *Robotics and Computer-Integrated Manufacturing* **2018**, *51*, 169–180. https://doi.org/10.1016/j.rcim.2017.12.005.
22. Ghaleb, A.M.; Kaid, H.; Alsamhan, A.; Mian, S.H.; Hidri, L. Assessment and Comparison of Various MCDM Approaches in the Selection of Manufacturing Process. *Advances in Materials Science and Engineering* **2020**, *2020*, 1–16. https://doi.org/10.1155/2020/4039253.
23. Wang, Y.; Zhong, R.Y.; Xu, X. A decision support system for additive manufacturing process selection using a hybrid multiple criteria decision-making method. *Rapid Prototyping Journal* **2018**, *24*, 1544–1553. https://doi.org/10.1108/rpj-01-2018-0002.
24. Wang, Y.C.; Chen, T.; Lin, Y.C. 3D Printer Selection for Aircraft Component Manufacturing Using a Nonlinear FGM and Dependency-Considered Fuzzy VIKOR Approach. *Aerospace* **2023**, *10*. https://doi.org/10.3390/aerospace10070591.
25. Grachev, D.I.; Chizhmakov, E.A.; Stepanov, D.Y.; Buslovich, D.G.; Khulaev, I.V.; Deshev, A.V.; Kirakosyan, L.G.; Arutyunov, A.S.; Kardanova, S.Y.; Panin, K.S.; et al. Dental Material Selection for the Additive Manufacturing of Removable Complete Dentures (RCD), 2023. https://doi.org/10.3390/ijms24076432.
26. Raigar, J.; Sharma, V.S.; Srivastava, S.; Chand, R.; Singh, J. A decision support system for the selection of an additive manufacturing process using a new hybrid MCDM technique. *Sādhanā* **2020**, *45*. https://doi.org/10.1007/s12046-020-01338-w.
27. Fera, M.; Macchiaroli, R.; Fruggiero, F.; Lambiase, A. A new perspective for production process analysis using additive manufacturing—complexity vs production volume. *The International Journal of Advanced Manufacturing Technology* **2018**, *95*, 673–685. https://doi.org/10.1007/s00170-017-1221-1.
28. Kalami, H.; Urbanic, J. Exploration of surface roughness measurement solutions for additive manufactured components built by multi-axis tool paths. *Additive Manufacturing* **2021**, *38*, 101822. https://doi.org/https://doi.org/10.1016/j.addma.2020.101822.
29. Un, U.N. Transforming our World: the 2030 Agenda for Sustainable Development. Report, eSocialSciences, 2015. Working Papers.
30. Rezaei, J. Best-worst multi-criteria decision-making method: Some properties and a linear model. *Omega* **2016**, *64*, 126–130. https://doi.org/10.1016/j.omega.2015.12.001.
31. GrabCAD. Bracket, 2023. Available online: https://grabcad.com/library/bracket-493 (accessed on 23-05-2024).
32. Pimenov, D.Y.; Kiran, M.; Khanna, N.; Pintaude, G.; Vasco, M.C.; da Silva, L.R.R.; Giasin, K. Review of improvement of machinability and surface integrity in machining on aluminum alloys. *The International Journal of Advanced Manufacturing Technology* **2023**, *129*, 4743–4779. https://doi.org/10.1007/s00170-023-12630-4.
33. Carpio, F.; Araújo, D.; Pacheco, F.; Méndez, D.; Garcìa, A.; Villar, M.; Garcìa, R.; Jiménez, D.; Rubio, L. Fatigue behaviour of laser machined 2024 T3 aeronautic aluminium alloy. *Applied Surface Science* **2003**, *208-209*, 194–198. https://doi.org/10.1016/S0169-4332(02)01369-7.
34. Giasin, K.; Hodzic, A.; Phadnis, V.; Ayvar-Soberanis, S. Assessment of cutting forces and hole quality in drilling Al2024 aluminium alloy: experimental and finite element study. *The International Journal of Advanced Manufacturing Technology* **2016**, *87*, 2041–2061. https://doi.org/10.1007/s00170-016-8563-y.
35. Ali, R.A.; Mia, M.; Khan, A.M.; Chen, W.; Gupta, M.K.; Pruncu, C.I. Multi-response optimization of face milling performance considering tool path strategies in machining of Al-2024. *Materials* **2019**, *12*, 1013. https://doi.org/10.3390/ma12071013.
36. Yücel, A.; Yildirim, c.V.; Sarikaya, M.; Şirin, c.; Kivak, T.; Gupta, M.K.; Tomaz, I.V. Influence of MoS2 based nanofluid-MQL on tribological and machining characteristics in turning of AA 2024 T3 aluminum alloy. *Journal of Materials Research and Technology* **2021**, *15*, 1688–1704. https://doi.org/10.1016/j.jmrt.2021.09.007.
37. UNI - Ente Italiano di Normazione, Milano, Italy. *Tolleranze generali. Tolleranze per dimensioni lineari ed angolari prive di indicazione di tolleranze specifiche.*, 1996. Available online: https://store.uni.com/uni-en-22768-1-1996 (accessed on 10-02-2024).
38. Samuel, A.; Araoyinbo, A.; Elewa, R.; Biodun, M. Effect of machining of aluminium alloys with emphasis on aluminium 6061 alloy–a review. In Proceedings of the IOP conference series: materials science and engineering. IOP Publishing, 2021, Vol. 1107, p. 012157. https://doi.org/10.1088/1757-899X/1107/1/012157.
39. Okokpujie, I.P.; Tartibu, L.K. A mini-review of the behaviour characteristic of machining processes of aluminium alloys. *Materials Today: Proceedings* **2022**, *62*, 4526–4532. https://doi.org/https://doi.org/10.1016/j.matpr.2022.05.006.
40. Zimmermann, N.; Müller, E.; Lang, S.; Mayr, J.; Wegener, K. Thermally compensated 5-axis machine tools evaluated with impeller machining tests. *CIRP Journal of Manufacturing Science and Technology* **2023**, *46*, 19–35. https://doi.org/https://doi.org/10.1016/j.cirpj.2023.07.005.
41. Liu, Y.; Xiong, S. Research Progress on Thermal Conductivity of High-Pressure Die-Cast Aluminum Alloys. *Metals* **2024**, *14*. https://doi.org/10.3390/met14040370.

42. Ye, W.; WU, S.p.; Xiang, X.; CHEN, R.r.; ZHANG, J.b.; XIAO, W.f. Formation mechanism and criterion of linear segregation in ZL205A alloy. *Transactions of Nonferrous Metals Society of China* **2014**, *24*, 3632–3638. https://doi.org/10.1016/S1003-6326(14)63508-1.
43. Jiang, H.; Zhang, L.; Zhao, B.; Sun, M.; He, M. Microstructure and Mechanical Properties of ZL205A Aluminum Alloy Produced by Squeeze Casting after Heat Treatment. *Metals* **2022**, *12*. https://doi.org/10.3390/met12122037.
44. Li, S.; Yue, X.; Li, Q.; Peng, H.; Dong, B.; Liu, T.; Yang, H.; Fan, J.; Shu, S.; Qiu, F.; et al. Development and applications of aluminum alloys for aerospace industry. *Journal of Materials Research and Technology* **2023**, *27*, 944–983. https://doi.org/https://doi.org/10.1016/j.jmrt.2023.09.274.
45. Goenka, M.; Nihal, C.; Ramanathan, R.; Gupta, P.; Parashar, A.; Joel, J. Automobile parts casting-methods and materials used: a review. *Materials Today: Proceedings* **2020**, *22*, 2525–2531. https://doi.org/10.1016/j.matpr.2020.03.381.
46. MRT, C. Casting Process, n.d. Available online: https://www.mrt-castings.co.uk/pressure-diecasting-methods.html#:~:text=High%20pressure%20die%20casting%20is,little%20as%201%2D2.5mm. (accessed on 23-05-2024).
47. Careri, F.; Khan, R.H.; Todd, C.; Attallah, M.M. Additive manufacturing of heat exchangers in aerospace applications: a review. *Applied Thermal Engineering* **2023**, *235*, 121387. https://doi.org/https://doi.org/10.1016/j.applthermaleng.2023.121387.
48. Martucci, A.; Aversa, A.; Lombardi, M. Ongoing Challenges of Laser-Based Powder Bed Fusion Processing of Al Alloys and Potential Solutions from the Literature—A Review. *Materials* **2023**, *16*. https://doi.org/10.3390/ma16031084.
49. Najafizadeh, M.; Yazdi, S.; Bozorg, M.; Ghasempour-Mouziraji, M.; Hosseinzadeh, M.; Zarrabian, M.; Cavaliere, P. Classification and applications of titanium and its alloys: A review. *Journal of Alloys and Compounds Communications* **2024**, *3*, 100019. https://doi.org/https://doi.org/10.1016/j.jacomc.2024.100019.
50. Rees, D.T.; Leung, C.L.A.; Elambasseril, J.; Marussi, S.; Shah, S.; Marathe, S.; Brandt, M.; Easton, M.; Lee, P.D. In situ X-ray imaging of hot cracking and porosity during LPBF of Al-2139 with TiB2 additions and varied process parameters. *Materials & Design* **2023**, *231*, 112031. https://doi.org/https://doi.org/10.1016/j.matdes.2023.112031.
51. Peddaiah, P.C.; Dodla, S. Experimental and numerical investigations of aerospace alloys: Effect of machining. *Proceedings of the Institution of Mechanical Engineers, Part E: Journal of Process Mechanical Engineering* **2024**. https://doi.org/10.1177/09544089241278080.
52. Rezaei, J. BWM solvers, n.d. Available online: https://bestworstmethod.com/software/ (accessed on 23-05-2024).
53. Kittur, J.K.; Manjunath Patel, G.; Parappagoudar, M.B. Modeling of pressure die casting process: an artificial intelligence approach. *International Journal of Metalcasting* **2016**, *10*, 70–87. https://doi.org/10.1007/s40962-015-0001-7.
54. Murugarajan, A.; Raghunayagan, P. The impact of pressure die casting process parameters on mechanical properties and its defects of A413 aluminium alloy. *Metalurgija* **2019**, *58*, 55–58.
55. Cao, L.; Li, J.; Hu, J.; Liu, H.; Wu, Y.; Zhou, Q. Optimization of surface roughness and dimensional accuracy in LPBF additive manufacturing. *Optics & Laser Technology* **2021**, *142*, 107246. https://doi.org/10.1016/j.optlastec.2021.107246.
56. Yang, T.; Liu, T.; Liao, W.; Wei, H.; Zhang, C.; Chen, X.; Zhang, K. Effect of processing parameters on overhanging surface roughness during laser powder bed fusion of AlSi10Mg. *Journal of Manufacturing Processes* **2021**, *61*, 440–453. https://doi.org/10.1016/j.jmapro.2020.11.030.
57. Priarone, P.C.; Ingarao, G.; Lunetto, V.; Di Lorenzo, R.; Settineri, L. The Role of re-design for Additive Manufacturing on the Process Environmental Performance. *Procedia CIRP* **2018**, *69*, 124–129. https://doi.org/10.1016/j.procir.2017.11.047.
58. Chen, N.; Barnawal, P.; Frank, M.C. Automated post machining process planning for a new hybrid manufacturing method of additive manufacturing and rapid machining. *Rapid Prototyping Journal* **2018**, *24*, 1077–1090. https://doi.org/10.1108/RPJ-04-2017-0057.
59. Fuchs, C.; Baier, D.; Semm, T.; Zaeh, M.F. Determining the machining allowance for WAAM parts. *Production Engineering* **2020**, *14*, 629–637. https://doi.org/10.1007/s11740-020-00982-9.
60. Ingarao, G.; Priarone, P.C.; Deng, Y.; Paraskevas, D. Environmental modelling of aluminium based components manufacturing routes: Additive manufacturing versus machining versus forming. *Journal of Cleaner Production* **2018**, *176*, 261–275. https://doi.org/10.1016/j.jclepro.2017.12.115.
61. Cecchel, S.; Cornacchia, G.; Panvini, A. Cradle-to-Gate Impact Assessment of a High-Pressure Die-Casting Safety-Relevant Automotive Component. *JOM* **2016**, *68*, 2443–2448. https://doi.org/10.1007/s11837-016-2046-3.
62. Liu, W.; Tang, R.; Peng, T. An IoT-enabled Approach for Energy Monitoring and Analysis of Die Casting Machines. *Procedia CIRP* **2018**, *69*, 656–661. https://doi.org/10.1016/j.procir.2017.11.109.
63. EOS GmbH. EOS M 290, n.d. Available online: https://www.eos.info/en-us/metal-solutions/metal-printers/data-sheets/sds-eos-m-290 (accessed on 10-08-2024).
64. EOS GmbH. EOS Aluminium AlSi2139 AM, n.d. Available online: https://www.eos.info/en-us/metal-solutions/metal-materials/aluminium#eos-aluminium-alsi10mg (accessed on 23-09-2024).
65. EOS GmbH. EOS Titanium Ti6Al4V, n.d. Available online: https://www.eos.info/en-us/metal-solutions/metal-materials/titanium#eos-titanium-ti64 (accessed on 23-09-2024).
66. Leal, R.; Barreiros, F.M.; Alves, L.; Romeiro, F.; Vasco, J.C.; Santos, M.; Marto, C. Additive manufacturing tooling for the automotive industry. *The International Journal of Advanced Manufacturing Technology* **2017**, *92*, 1671–1676. https://doi.org/10.1007/s00170-017-0239-8.

67. Sgarbossa, F.; Peron, M.; Lolli, F.; Balugani, E. Conventional or additive manufacturing for spare parts management: An extensive comparison for Poisson demand. *International Journal of Production Economics* **2021**, *233*, 107993. https://doi.org/10.1016/j.ijpe.2020.107993.
68. Atzeni, E.; Salmi, A. Economics of additive manufacturing for end-usable metal parts. *The International Journal of Advanced Manufacturing Technology* **2012**, *62*, 1147–1155. https://doi.org/10.1007/s00170-011-3878-1.
69. 3D Natives. A Comprehensive List of All the Metal 3D Printer Manufacturers, n.d. Available online: https://www.3dnatives.com/en/metal-3d-printer-manufacturers/ (accessed on 12-08-2024).
70. 3D SYSTEMS. DMP Flex 200, n.d. Available online: https://www.3dsystems.com/3d-printers/dmp-flex-200 (accessed on 12-08-2024).
71. 3D SYSTEMS. DMP Factory 350, n.d. Available online: https://www.3dsystems.com/3d-printers/dmp-factory-350 (accessed on 12-08-2024).
72. 3D SYSTEMS. DMP Flex 350, n.d. Available online: https://www.3dsystems.com/3d-printers/dmp-flex-350 (accessed on 12-08-2024).
73. 3D SYSTEMS. DMP Factory 500, n.d. Available online: https://www.3dsystems.com/3d-printers/dmp-factory-500 (accessed on 12-08-2024).
74. Colibrium Additive. M2 Series 5, n.d. Available online: https://www.colibriumadditive.com/printers/l-pbf-printers/m2-series-5 (accessed on 10-08-2024).
75. Colibrium Additive. X Line 2000R, n.d. Available online: https://www.colibriumadditive.com/printers/l-pbf-printers/x-line-2000r (accessed on 10-08-2024).
76. Colibrium Additive. M Line, n.d. Available online: https://www.colibriumadditive.com/printers/l-pbf-printers/m-line (accessed on 10-08-2024).
77. DMG MORI. LASERTEC 12 SLM, n.d. Available online: https://uk.dmgmori.com/products/machines/additive-manufacturing/powder-bed/lasertec-12-slm (accessed on 10-08-2024).
78. DMG MORI. LASERTEC 30 DUAL SLM, n.d. Available online: https://uk.dmgmori.com/products/machines/additive-manufacturing/powder-bed/lasertec-30-slm?_gl=1*l463zu*_gcl_au*MTc2NjEwMDMxNi4xNzIyOTMxNDcy*_ga*MTU4NDc1MjA5Ny4xNzIyOTMxNDcz*_ga_XQ3E6CJXX5*MTcyMzU2NjY4Ni4yLjEuMTcyMzU2NzY3OS41MS4wLjA. (accessed on 10-08-2024).
79. EOS GmbH. EOS M 300-4, n.d. Available online: https://uk.eos.info/en-gb/industrial-3d-printer/metal/eos-m-300-4 (accessed on 10-08-2024).
80. EOS GmbH. EOS M 400, n.d. Available online: https://uk.eos.info/en-gb/industrial-3d-printer/metal/eos-m-400 (accessed on 10-08-2024).
81. EOS GmbH. EOS M 400-4, n.d. Available online: https://uk.eos.info/en-gb/industrial-3d-printer/metal/eos-m-400-4 (accessed on 10-08-2024).
82. Farsoon Technologies. FS121M, n.d. Available online: https://www.farsoon-gl.com/products/fs121m/ (accessed on 10-08-2024).
83. Farsoon Technologies. FS273M, n.d. Available online: https://www.farsoon-gl.com/products/fs273m/ (accessed on 10-08-2024).
84. Farsoon Technologies. FS200M, n.d. Available online: https://www.farsoon-gl.com/products/fs200m/ (accessed on 10-08-2024).
85. Farsoon Technologies. FS301M, n.d. Available online: https://www.farsoon-gl.com/products/fs301m/ (accessed on 10-08-2024).
86. Farsoon Technologies. FS350M-4, n.d. Available online: https://www.farsoon-gl.com/products/fs350m-4/ (accessed on 10-08-2024).
87. Farsoon Technologies. FS422M, n.d. Available online: https://www.farsoon-gl.com/products/fs422m/ (accessed on 10-08-2024).
88. Farsoon Technologies. FS721M-CAMS, n.d. Available online: https://www.farsoon-gl.com/products/fs721m-cams/ (accessed on 10-08-2024).
89. Farsoon Technologies. FS721M, n.d. Available online: https://www.farsoon-gl.com/products/fs721m/ (accessed on 10-08-2024).
90. Farsoon Technologies. FS621M, n.d. Available online: https://www.farsoon-gl.com/products/fs621m/ (accessed on 10-08-2024).
91. Matsuura Machinery. LUMEX Avance-25, n.d. Available online: https://www.lumex-matsuura.com/english/lumex-avance-25 (accessed on 10-08-2024).
92. Matsuura Machinery. LUMEX Avance-60, n.d. Available online: https://www.lumex-matsuura.com/english/lumex-avance-60 (accessed on 10-08-2024).
93. Prima Additive. Print Sharp 150, n.d. Available online: https://www.primaadditive.com/en/technologies/powder-bed-fusion/print-sharp-150 (accessed on 10-08-2024).
94. Prima Additive. Print Genius 150, n.d. Available online: https://www.primaadditive.com/en/technologies/powder-bed-fusion/print-genius-150 (accessed on 10-08-2024).
95. Prima Additive. Print Green, n.d. Available online: https://www.primaadditive.com/en/technologies/powder-bed-fusion/print-green-150 (accessed on 10-08-2024).
96. Prima Additive. 300 Family, n.d. Available online: https://www.primaadditive.com/en/technologies/powder-bed-fusion/300-family (accessed on 10-08-2024).
97. Prima Additive. Print Genius 400, n.d. Available online: https://www.primaadditive.com/en/technologies/powder-bed-fusion/print-genius-400 (accessed on 10-08-2024).

98. Renishaw. RenAM 500, n.d. Available online: https://www.renishaw.com/en/renam-500-metal-additive-manufacturing-3d-printing-systems--37011 (accessed on 10-08-2024).
99. SLM Solutions. SLM 125, n.d. Available online: https://slm-solutions.com/products-and-solutions/machines/slm-125/ (accessed on 10-08-2024).
100. SLM Solutions. SLM 280 PS, n.d. Available online: https://www.slm-solutions.com/products-and-solutions/machines/slm-280-production-series/ (accessed on 10-08-2024).
101. SLM Solutions. SLM 280 2.0, n.d. Available online: https://www.slm-solutions.com/products-and-solutions/machines/slm-280/ (accessed on 10-08-2024).
102. SLM Solutions. SLM 500, n.d. Available online: https://www.slm-solutions.com/products-and-solutions/machines/slm-500/ (accessed on 10-08-2024).
103. SLM Solutions. SLM 800, n.d. Available online: https://www.slm-solutions.com/products-and-solutions/machines/slm-800/ (accessed on 10-08-2024).
104. SLM Solutions. SLM NXG XII 600, n.d. Available online: https://www.slm-pushing-the-limits.com/ (accessed on 10-08-2024).
105. Sharebot. metalONE, n.d. Available online: https://sharebot.us/metalone/ (accessed on 10-08-2024).
106. TRUMPF. TruePrint 1000, n.d. Available online: https://www.trumpf.com/en_GB/products/machines-systems/additive-production-systems/truprint-1000/ (accessed on 10-08-2024).
107. TRUMPF. TruePrint 1000 Basic Edition, n.d. Available online: https://www.trumpf.com/en_GB/products/machines-systems/additive-production-systems/truprint-1000-basic-edition/ (accessed on 10-08-2024).
108. TRUMPF. TruePrint 2000, n.d. Available online: https://www.trumpf.com/en_GB/products/machines-systems/additive-production-systems/truprint-2000/ (accessed on 10-08-2024).
109. TRUMPF. TruePrint 3000, n.d. Available online: https://www.trumpf.com/en_GB/products/machines-systems/additive-production-systems/truprint-3000/ (accessed on 10-08-2024).
110. TRUMPF. TruePrint 5000, n.d. Available online: https://www.trumpf.com/en_GB/products/machines-systems/additive-production-systems/truprint-5000/ (accessed on 10-08-2024).
111. TRUMPF. TruePrint 5000 Green Edition, n.d. Available online: https://www.trumpf.com/en_GB/products/machines-systems/additive-production-systems/truprint-5000-green-edition/ (accessed on 10-08-2024).
112. Velo3D. Sapphire and Sapphire 1MZ Printers, n.d. Available online: https://velo3d.com/product-brief-sapphire-and-sapphire-1mz-printer/ (accessed on 10-08-2024).
113. Velo3D. Sapphire XC and Sapphire XC 1MZ Printers, n.d. Available online: https://velo3d.com/products/#sapphire (accessed on 10-08-2024).

Disclaimer/Publisher's Note: The statements, opinions and data contained in all publications are solely those of the individual author(s) and contributor(s) and not of MDPI and/or the editor(s). MDPI and/or the editor(s) disclaim responsibility for any injury to people or property resulting from any ideas, methods, instructions or products referred to in the content.